Gamma-irradiation degraded sulfated polysaccharide from a new red algal strain *Pyropia yezoensis* Sookwawon 104 with *in vitro* antiproliferative activity

DAN HE[1,2*], LIPING YAN[1*], XIAOJING MA[3], YANG CHENG[1], SIYA WU[1], JIHUI ZUO[1], EUN-JEONG PARK[4], JIAN LIU[1,2], MINGJIANG WU[1], JONG-IL CHOI[2] and HAIBIN TONG[1]

[1]Zhejiang Provincial Key Laboratory for Water Environment and Marine Biological Resources Protection, College of Life and Environmental Science, Wenzhou University, Wenzhou, Zhejiang 325035, P.R. China; [2]Department of Biotechnology and Bioengineering, Chonnam National University, Gwangju 61186, Republic of Korea; [3]National Resource Center of Chinese Materia Medica, China Academy of Chinese Medical Sciences, Beijing 100700, P.R. China; [4]Seaweed Research Center, National Institute of Fisheries Science, Haenam, South Jeolla 59002, Republic of Korea

Received September 17, 2019; Accepted July 21, 2020

DOI: 10.3892/ol.2020.11952

Abstract. *Pyropia yezoensis* Sookwawon 104 is a newly cultivated strain of red marine algae. The present study aimed to investigate the *in vitro* antiproliferative activity of sulfated polysaccharide extracted from *P. yezoensis* Sookwawon 104 (PYSP), as well as that of its low molecular weight (Mw) derivatives. PYSP is a heterogeneous sulfated polysaccharide mainly composed of galactose, glucose and fucose. PYSP was degraded by gamma-irradiation at doses of 20 and 100 kGy to produce two derivatives, named as PYSP-20 and PYSP-100, respectively. Comparison of PYSP, PYSP-20 and PYSP-100 revealed clear differences in their molecular weight (Mw) distributions, and distinct *in vitro* antiproliferative activities against Hep3B, MDA-MB-231 and HeLa cancer cell lines. PYSP-20 and PYSP-100 exhibited stronger antiproliferative effects than PYSP, suggesting that the reduction in Mw may have increased the *in vitro* antiproliferative activity. Furthermore, the mRNA expression levels of the antitumor gene *P53* and cell cycle-associated genes *P21*, Cyclin B1 and cyclin dependent kinase 1 (*Cdk1*) were further analyzed by reverse transcription-quantitative PCR in PYSP-20 and PYSP-100-treated cancer cells. PYSP and its derivatives were shown to inhibit the proliferation of tumor cells by regulating the expression of *P53*, *P21*, Cyclin B1 and *Cdk1*. In conclusion, low-Mw polysaccharide derivatives prepared from *P. yezoensis* Sookwawon 104 by gamma-irradiation exhibit significant inhibition effects on cancer cell proliferation *in vitro* and may be a novel source of potential anticancer therapeutic agents.

Correspondence to: Professor Haibin Tong, Zhejiang Provincial Key Laboratory for Water Environment and Marine Biological Resources Protection, College of Life and Environmental Science, Wenzhou University, 586, Meiquan Street, Chashan Town, Wenzhou, Zhejiang 325035, P.R. China
E-mail: tonghaibin@gmail.com

Professor Jong-Il Choi, Department of Biotechnology and Bioengineering, Chonnam National University, 77 Yongbong-ro, Buk-gu, Gwangju 61186, Republic of Korea
E-mail: choiji01@chonnam.ac.kr

*Contributed equally

Key words: Pyropia yezoensis, sulfated polysaccharide, gamma-irradiation, antitumor

Introduction

Pyropia yezoensis (*Porphyra yezoensis; P yezoensis*) is an edible marine red alga containing various biological macromolecules, such as sulfated polysaccharides, which have antioxidant, anti-inflammatory, antitumor and immunomodulatory activity (1-5). The anticancer bioactivities and applications of natural polysaccharides are of considerable interest to researchers and have been investigated using *in vivo* and *in vitro* models. For example, *Porphyra haitanensis* polysaccharide exhibited an antiproliferative effect on the GC7901 human gastric cancer cell line via the induction of cell apoptosis, and demonstrated an *in vivo* antitumor effect on SGC7901 tumor-bearing mice (6). An ultrasound-degraded polysaccharide from *P. yezoensis* also demonstrated significant inhibitory activity in SGC7901 cells (2). In addition, an agar-type sulfated polysaccharide derived from *Gracilaria dominguensis* inhibited Ehrlich ascites carcinoma in mice (7). Furthermore, a sulfated polysaccharide from *Champia feldmannii* (Diaz-Pifferer) inhibited sarcoma 180 tumors in mice (8). These previous studies indicate that various sulfated polysaccharides isolated from red algae have the potential to be used as natural antitumor agents due to their effectiveness in inhibiting the proliferation of tumor cells *in vitro* and *in vivo*.

There is also evidence to suggest that oligosaccharides and polysaccharides derived from seaweed are beneficial for

human health and may have a wide range of applications (9). In a review by Cheong *et al* (10), the notable biological activity of oligosaccharides from red seaweed was suggested to support their development for use in functional foods and the pharmaceutical industry. Therefore, polysaccharides, oligosaccharides and their derivates are of great interest to researchers. There are a number of reports concerning the use of polysaccharides with low molecular weight (Mw) to treat cancer in clinical trials, with these polysaccharides including glucan-based oligosaccharides, heparan sulfate mimetics and inulin/oligofructose (11-13). Low-Mw polysaccharides are generally prepared by methods including acid hydrolysis, ultrasonic degradation, an ascorbic acid/H_2O_2 redox system, enzymatic degradation, microwave-assisted acid hydrolysis and gamma-irradiation (2,14-17). The use of different degradation methods may help to broaden the scope of the polysaccharides.

The present study aimed to expand the antitumor applications of sulfated polysaccharides isolated from algae, and also to elucidate the characteristics and bioactivity of some degraded derivatives obtained using gamma-irradiation. Specifically, a sulfated polysaccharide was extracted from the newly cultivated strain *P. yesoensis* Sookwawon 104 by dilute hydrochloric acid extraction, and low-Mw polysaccharides were prepared from it by gamma-irradiation (20 and 100 kGy). The *in vitro* antiproliferative activity of the *P. yezoensis* sulfated polysaccharide (PYSP) and its derivatives on three tumor cell lines, namely the HeLa human cervical cancer cell line, MDA-MB-231 human breast carcinoma cell line and Hep3B human hepatic carcinoma cell line, and their potential mechanisms were also investigated.

Materials and methods

Materials and chemicals. The algal specimen *P. yezoensis* Sookwawon 104 was collected by the National Institute of Fisheries Science (South Korea). The specimen was identified by EJP and deposited at the Seaweed Research Center (South Korea) with the voucher specimen number Sookwawon 104. Thiazolyl blue tetrazolium bromide (MTT) were purchased from BBI Life Sciences Corporation. Mannose, rhamnose, glucuronic acid, galacturonic acid, glucose, galactose, xylose, arabinose and fucose were obtained from the Sinopharm Chemical Reagent Co. Ltd for the monosaccharide composition analysis. TransScript All-in-One First-Strand cDNA Synthesis SuperMix and TransStart® Top Green qPCR SuperMix were purchased from Beijing TransGen Biotech Co., Ltd. Dulbecco's modified Eagle's medium (DMEM), Leibovitz's L-15 medium and fetal bovine serum (FBS) were purchased from Gibco (Thermo Fisher Scientific, Inc.). Penicillin-streptomycin solution (100X) was obtained from Biosharp Life Sciences. All other chemical reagents used were of analytical grade.

Extraction of P. yezoensis polysaccharide. Dried and powdered *P. yezoensis* Sookwawon 104 (50 g) was passed through a 40-mesh sieve. Fat and pigment were then removed by refluxing with 250 ml 95% ethanol at 60˚C for 6 h. The residue (45 g) was extracted twice with 1 mM HCl (1.3 l) at 80˚C for 2 h. After filtration, the supernatant was concentrated to 0.65 l using a rotary evaporator at 50˚C. Then, 95% ethanol (2.6 l) was added to the concentrate which was maintained at 4˚C overnight. Following centrifugation at 2,000 x g for 10 min at room temperature, the precipitate, named PYSP, was collected and dried in a vacuum drying oven at 70˚C (18).

Preparation of degradation derivatives by gamma-irradiation. PYSP (5% in water, w/v; pH 7.0) was degraded by gamma-irradiation at doses of 20 and 100 kGy, respectively, as previously described (15). The degradation derivatives were collected, lyophilized in a vacuum and freeze-dried. The derivatives obtained using 20 and 100 Gy were named as PYSP-20 and PYSP-100, respectively.

Component analysis. PYSP and its degradation derivatives were subjected to component analysis. The total sugar content was detected using the phenol-sulfuric acid method (19). The protein content was analyzed using the Bradford method (20). The sulfate group content was determined using a turbidimetric method (21).

Monosaccharide composition analysis. The monosaccharide compositions of PYSP, PYSP-20 and PYSP-100 were analyzed by high-performance liquid chromatography using a 1-phenyl-3-methyl-5-pyrazolone (PMP) pre-column derivatization method (22). Briefly, the samples were hydrolyzed with 2 M trifluoroacetic acid at 100˚C for 4 h. Excess acid was removed by adding ethanol at 60˚C, and then NaOH (0.3 M, 300 μl) and PMP (0.5 M, 300 μl) were added to the reaction mixture, which was subsequently incubated at 70˚C for another 1 h. Following neutralization by the addition of 0.3 M HCl, chloroform (1 ml) was added to the reaction mixture. The aqueous phase of three samples (20 μl) was analyzed by Waters 1525 HPLC system (Waters Corporation; https://www.waters.com/nextgen/us/en.html) on a Hypersil ODS-2 column (5 μm, 4.6x250 mm; Thermo Fisher Scientific Inc.) at a flow rate of 0.8 ml/min. The mobile phases were 0.05 M phosphate buffer solution (pH 6.8) and acetonitrile (83:17, v/v), and the detection wavelength was 254 nm at 25˚C. Different monosaccharide standards (mannose, fucose, xylose, galactose, glucose, arabinose, rhamnose, galacturonic acid and glucuronic acid) were used to analyze the monosaccharide composition of PYSP and its derivatives.

Mw analysis. The Mw distributions of PYSP, PYSP-20 and PYSP-100 were measured by high-performance gel permeation chromatography. Dextran standards with different molecular weights (2,000, 150, 41.1, 21.4, 7.1 and 4.6 kDa, and 180 Da) were used to calibrate the column and establish a standard curve using linear regression (22). Each sample, dissolved in 0.1 M Na_2SO_4 solution, was analyzed using a TSK-GEL G5000 PWXL column (7.8x300 mm; Tosoh Corporation) and Waters 2424 Refractive Index Detector (Waters Corporation), which was eluted with 0.1 M Na_2SO_4 solution.

Fourier transform-infrared (FT-IR) analysis. Each sample (4 mg) was mixed with KBr powder (0.4 g), pressed into pellets and analyzed using an Infrared Spectrometer TENSOR 27 (Bruker Corporation) at the frequency range from 400 to 4,000 cm^{-1} (23).

Cell culture. HeLa, Hep3B and MDA-MB-231 cells were purchased from the Cell Bank of Shanghai Institute of

Table I. Mw distributions and chemical compositions of PYSP and its derivatives.

Sample	Carbohydrate (%)	Mw (kDa)	Protein (%)	Sulfate (%)	Molar ratio of monosaccharides		
					Glc	Gal	Fuc
PYSP	83.6±1.63	3,315; 137; 8	0.83±0.03	12.2±0.07	1.6	17.9	1.0
PYSP-20	83.0±1.66	172; 44; 8	0.42±0.07	12.7±0.15	2.0	17.6	1.0
PYSP-100	83.0±1.55	25.8; 8	0.38±0.08	12.6±0.37	1.7	13.5	1.0

PYSP, sulfated polysaccharide extracted from *P. yezoensis* Sookwawon 104; PYSP-20, degradation product of PYSP obtained using 20 kGy gamma-irradiation; PYSP-100, degradation product of PYSP obtained using 100 kGy gamma-irradiation; Mw, molecular weight; gal, galactose; fuc, fucose; glc, glucose. Data are presented as the mean ± standard deviation (n=3).

Biochemistry and Cell Biology. The HeLa and Hep3B cells were maintained in DMEM, and the MDA-MB-231 cells were maintained in L-15 medium. All media were supplemented with 10% FBS and antibiotics (100 U/ml penicillin and 100 μg/ml streptomycin). The cell cultures were incubated at 37˚C in a humidified atmosphere containing 5% CO_2.

MTT assay. Hep3B, HeLa and MDA-MB-231 cells were each seeded in 96-well plates at a density of $3x10^3$ cells/well in 200 μl medium. The cells were treated with PYSP, PYSP-20 or PYSP-100 at concentrations of 200 or 500 μg/ml at 37˚C for 48 h. Then, 20 μl MTT (5 mg/ml) was added to each well, and the cells were incubated for another 4 h. Finally, the cell viability was detected as previously described (24). The inhibition rate was calculated from the optical density (OD) at 490 nm using the following formula: Inhibition rate (%) = $(1-OD_{treatment}/OD_{untreated})$ x100.

Crystal violet assay. Hep3B, HeLa and MDA-MB-231 cells were seeded in 24-well plates at a density of $5x10^4$ cells/well in 1 ml medium overnight and then treated with PYSP-20 or PYSP-100 at 200 or 500 μg/ml at 37˚C for 48 h. Untreated cells served as the control. The cells were then fixed with 4% paraformaldehyde at 25˚C for 30 min, stained with 0.1% crystal violet for 30 min at room temperature, and then washed with distilled water. Finally, 10% acetic acid was added to each well and the absorbance at 595 nm was measured using a Cytation 3 microplate reader (BioTek Instruments, Inc.). The relative proliferation rate was calculated using the following formula: Relative proliferation rate = $OD_{treatment}/OD_{untreated}$.

Reverse transcription-quantitative PCR (RT-qPCR). Hep3B, HeLa and MDA-MB-231 cells were seeded in 24-well plates at a density of $5x10^4$ cells/well in 1 ml medium overnight and then treated with PYSP-20 or PYSP-100 at 200 μg/ml at 37˚C for 48 h. The cells were then collected and total RNA was extracted from them using TRIzol reagent (Invitrogen; Thermo Fisher Scientific, Inc.). RNA (2 μg/μl) was used for cDNA synthesis using TransScript All-in-One First-Strand cDNA Synthesis SuperMix. The cDNA samples were used as the template for the qPCR reaction using gene-specific primers. The final reaction volume of 10 μl contained 5 μl TransStart® Top Green qPCR SuperMix, 0.5 μl forward and reverse primers and 1 μl cDNA template. qPCR was conducted using a LightCycler 480 Instrument II (Roche Applied Science). The PCR thermocycling conditions were as follows: 1 cycle at 95˚C for 30 sec followed by 40 cycles at 95˚C for 30 sec, 58˚C for 30 sec and 72˚C for 20 sec. The relative amounts of mRNA were calculated using the $2^{-\Delta\Delta Cq}$ method (25). The primer sequences were as follows: *P53*, forward: 5'-CCCCTCCTGGCCCCTGTCATCTTC-3' and reverse: 5'-GCAGCGCCTCACAACCTCCGTCAT-3'; *P21*, forward: 5'-GCGGAACAAGGAGTCAGACA-3' and reverse: 5'-GAACCAGGACACATGGGGAG-3'; Cyclin B1, forward: 5'-CTGCTGGGTGTAGGTCCTTG-3' and reverse: 5'-TGC CATGTTGATCTTCGCCT-3'; *Cdk1*, forward: 5'-TTGAAA CTGCTCGCACTTGG-3' and reverse: 5'-TCCCGGCTTATT ATTCCGCG-3'; *GAPDH*, forward: 5'-GCAGGGGGGAGC CAAAAGGGT-3' and reverse: 5'-TGGGTGGCAGTGATG GCATGG-3'. *GAPDH* served as an internal reference.

Statistical analysis. Data are expressed as means ± standard deviation. GraphPad Prism 5.0 (GraphPad Software, Inc.) and Origin 8.5 (OriginLab Corporation) were used to prepare graphs and for analysis of the data using one-way and two-way ANOVA analysis of variance followed by Tukey's post hoc test. $P<0.05$ was considered to indicate a statistically significant difference.

Results

Characterization of the polysaccharides. Extraction of 50 g dried *P. yezoensis* Sookwawon 104 using diluted hydrochloric acid extraction and ethanol precipitation yielded 5 g PYSP. The carbohydrate content, Mw and chemical composition of PYSP and its degradation products are shown in Table I. PYSP, PYSP-20 and PYSP-100 were composed of galactose, fucose and glucose in a molar ratio of 1.6:17.9:1.0, 2.0:17.6:1.0 and 1.7:13.5:1.0, respectively. The chemical compositions of PYSP, PYSP-20, and PYSP-100 were not markedly different; however, the Mw distribution was clearly reduced when the dose of gamma-irradiation was increased (Fig. 1). The FT-IR spectrum (Fig. 2) of each sample revealed a major broad stretching peak at ~3,430 cm^{-1} for the hydroxyl group, and a weak band at ~2,930 cm^{-1} for the C-H stretching vibration. The peak at 931 cm^{-1} indicated the existence of

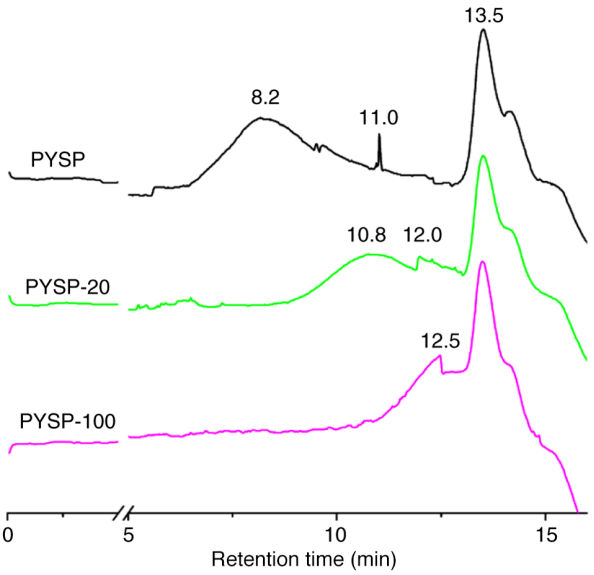

Figure 1. Molecular weight distribution of PYSP, PYSP-20 and PYSP-100 determined using high-performance gel permeation chromatography. The curves are displaced vertically to avoid overlap. PYSP, sulfated polysaccharide extracted from *P. yezoensis* Sookwawon 104; PYSP-20, degradation product of PYSP obtained using 20 kGy gamma-irradiation; PYSP-100, degradation product of PYSP obtained using 100 kGy gamma-irradiation.

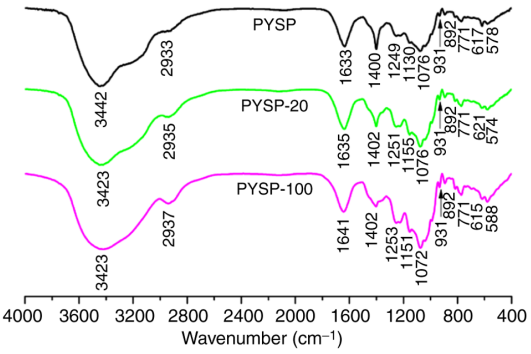

Figure 2. Fourier transform-infrared spectra of PYSP, PYSP-20 and PYSP-100. The spectra are displaced vertically to avoid overlap. PYSP, sulfated polysaccharide extracted from *P. yezoensis* Sookwawon 104; PYSP-20, degradation product of PYSP obtained using 20 kGy gamma-irradiation; PYSP-100, degradation product of PYSP obtained using 100 kGy gamma-irradiation.

an ether bond (-C-O-C-), suggesting all samples contained 3,6-anhydro-α-L-galactose (14). The signals presented at ~1,250 and 890 cm^{-1} were respectively caused by the stretching vibrations of S=O and C-O-S groups (26,27), indicating that all samples contained sulfate groups. The peaks near 1,635 and 1,400 cm^{-1} observed for PYSP, PYSP-20 and PYSP-100 were the stretching vibrations of carboxyl and carbonyl groups (28). Together, the composition analysis and FT-IR spectra confirmed that PYSP and its derivatives did not exhibit any marked differences, with the exception of Mw distribution.

Antiproliferative activity. The *in vitro* antiproliferative effects of PYSP, PYSP-20 and PYSP-100 on Hep3B, HeLa and MDA-MB-231 cells were analyzed using MTT and crystal violet assays. As shown in Fig. 3, PYSP-20 and PYSP-100 exhibited marked antiproliferative effects on MDA-MB-231 cells, whereas PYSP had weaker antiproliferative activity. PYSP-20 and PYSP-100 displayed inhibition rates of 40-50% in MDA-MB-231 cells. Notably, the inhibition rate for PYSP-20 at a concentration of 500 μg/ml reached 50.6% (Fig. 3C). According to the results of the crystal violet assay, the relative proliferation rate of the cells decreased by almost half following treatment with PYSP-20 or PYSP-100 (Fig. 3A and B). The effects of PYSP, PYSP-20 and PYSP-100 on HeLa cells are shown in Fig. 4. PYSP-20 and PYSP-100 at concentrations of 200 and 500 μg/ml exhibited notable antiproliferative effects against HeLa cells, with a maximum inhibition rate of ~50% (Fig. 4C). However, PYSP exhibited an antiproliferative effect only at 200 μg/ml. Consistent with the results of the MTT assay, the relative proliferation rates of HeLa cells treated with PYSP-20 or PYSP-100 determined using the crystal violet assay (Fig. 4A and B) exhibited a similar inhibitory trend as those of the MTT assay in Fig. 4C. In Hep3B cells, PYSP, PYSP-20 and PYSP-100 exhibited antiproliferative effects at concentrations of 200 and 500 μg/ml. and their inhibition rate reached ~50%. The inhibition rate of PYSP-100 was significantly higher than that of PYSP or PYSP-20 at the concentration of 500 μg/ml (Fig. 5C). Also, the relative proliferation rates of PYSP-20 and PYSP-100 were been reduced by almost half compared with those in the control group (Fig. 5A and B).

Due to the greater *in vitro* antiproliferative activity of PYSP-20 and PYSP-100 when compared with PYSP, their potential antiproliferative mechanism was further explored through measuring the expression of genes regulating the cell cycle, namely Cyclin B1, *Cdk1*, *P53* and *P21* (Fig. 6). The treatment of Hep3B cells with PYSP-20 or PYSP-100 appeared to reduce the mRNA levels of cyclin B1 and *Cdk1* compared with those in the control group, while the expression levels of *P53* and *P21* significantly increased. In HeLa cells, *Cdk1* was significantly decreased after PYSP-20 treatment. Furthermore, *P53* and *P21* in HeLa cells appeared to be upregulated following PYSP-20 or PYSP-100 treatment, with *P21* exhibiting a significant increase in response to treatment with PYSP-20. In the MDA-MB-231 cells, Cyclin B1 and *Cdk1* appeared to be slightly downregulated after PYSP-20 or PYSP-100 treatment. Moreover, PYSP-20 exposure significantly increased the mRNA levels of *P21*, while PYSP-100 significantly increased the mRNA levels of *P53* expression in MDA-MB-231 cells.

Discussion

Red algae is an abundant marine resource that comprises various species, including *Gracilaria gracili* and *P. yezoensis*. *P. yezoensis* contains multiple bioactive macromolecules, including polysaccharides, proteins and polyunsaturated fatty acids (29). In the present study, the polysaccharide PYSP was extracted from a new red alga strain *P. yezoensis* Sookwawon 104 and the degradation derivatives PYSP-20 and PYSP-100 were prepared by gamma-irradiation. The antiproliferative activities of these polysaccharides were investigated *in vitro* against Hep3B, HeLa and MDA-MB-231 cells. In the Mw analysis, the elution curve indicated that PYSP mainly comprises high-Mw polysaccharide. Since the available evidence shows that the reduction of Mw may improve the

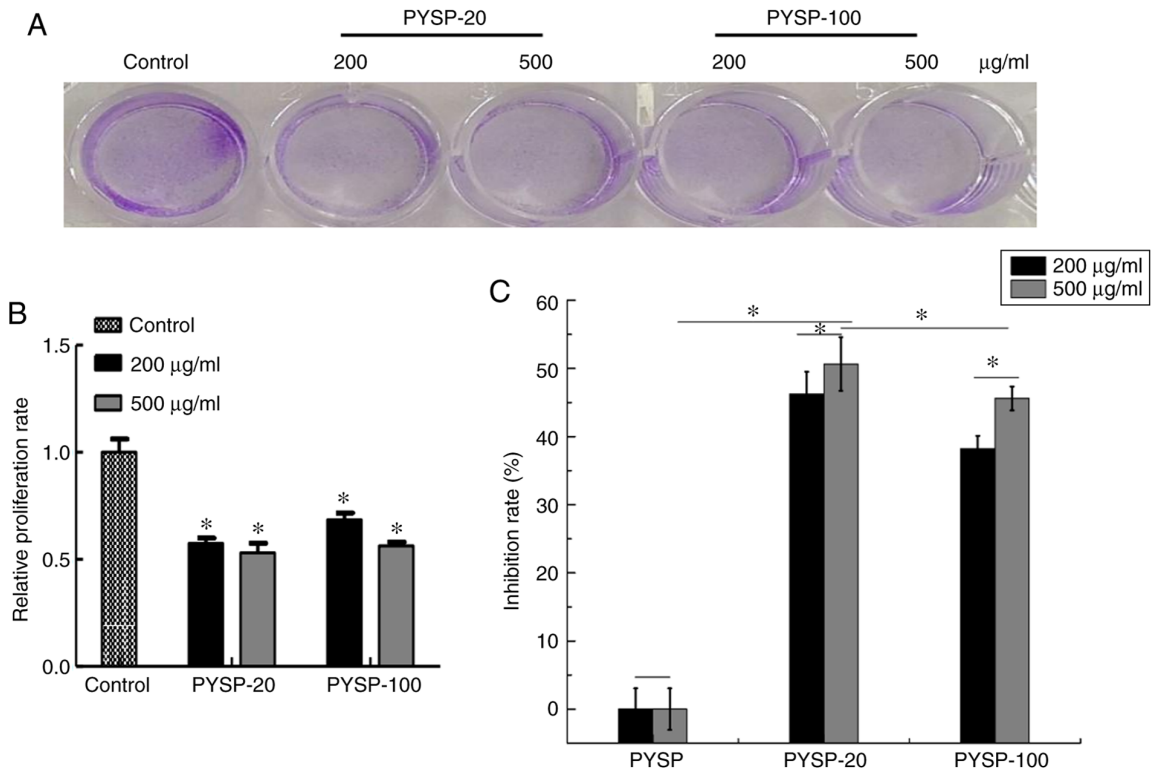

Figure 3. Effects of polysaccharides on MDA-MB-231 cell proliferation. (A) Crystal violet staining images. (B) Relative proliferation rate, as measured by crystal violet staining (n=3). Stastical analysis was performed using one-way ANOVA followed by Tukey's post hoc test. *P<0.05 vs. control. (C) Inhibition rate as measured by MTT assay. Data are the means ± SD (n=3). Stastical analysis was performed using two-way ANOVA followed by Tukey's post hoc test. *P<0.05. PYSP, sulfated polysaccharide extracted from *P. yezoensis* Sookwawon 104; PYSP-20, degradation product of PYSP obtained using 20 kGy gamma-irradiation; PYSP-100, degradation product of PYSP obtained using 100 kGy gamma-irradiation.

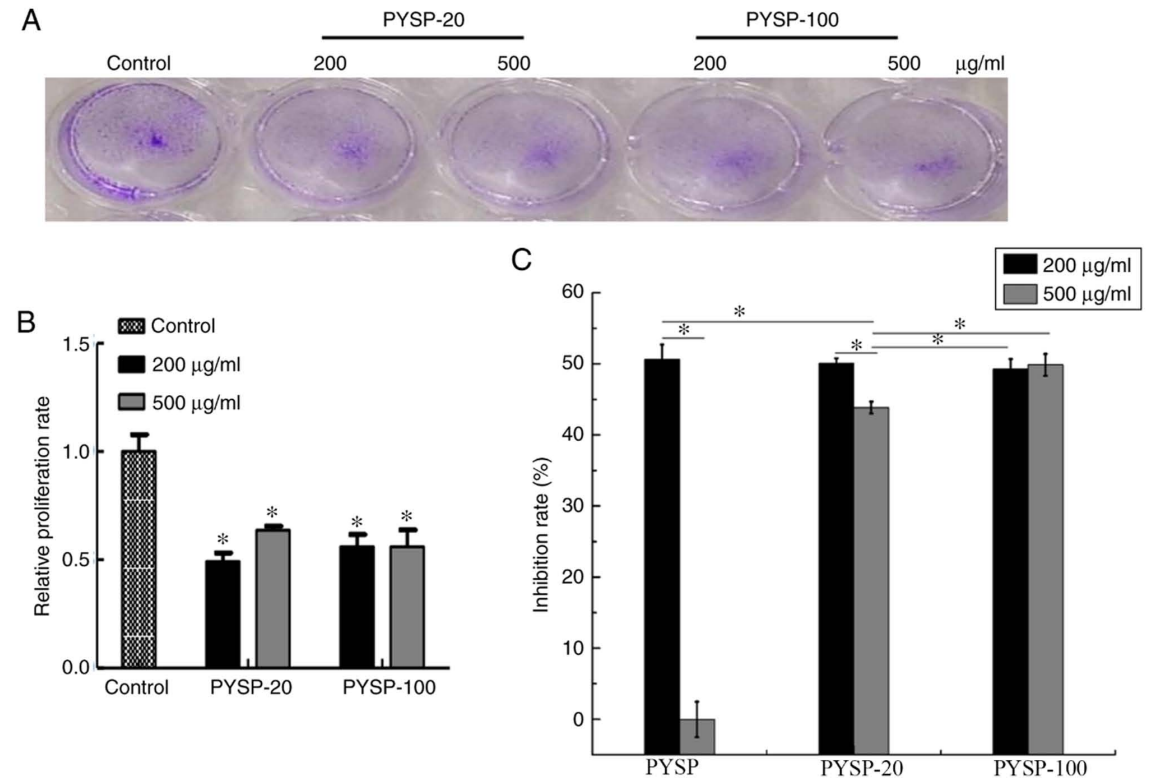

Figure 4. Effects of polysaccharides on HeLa cell proliferation. (A) Crystal violet staining images. (B) Relative proliferation rate, as measured by crystal violet staining (n=3). Stastical analysis was performed using one-way ANOVA followed by Tukey's post hoc test. *P<0.05 vs. control. (C) Inhibition rate as measured by MTT assay. Data are the means ± SD (n=3). Stastical analysis was performed using two-way ANOVA followed by Tukey's post hoc test. *P<0.05. PYSP, sulfated polysaccharide extracted from *P. yezoensis* Sookwawon 104; PYSP-20, degradation product of PYSP obtained using 20 kGy gamma-irradiation; PYSP-100, degradation product of PYSP obtained using 100 kGy gamma-irradiation.

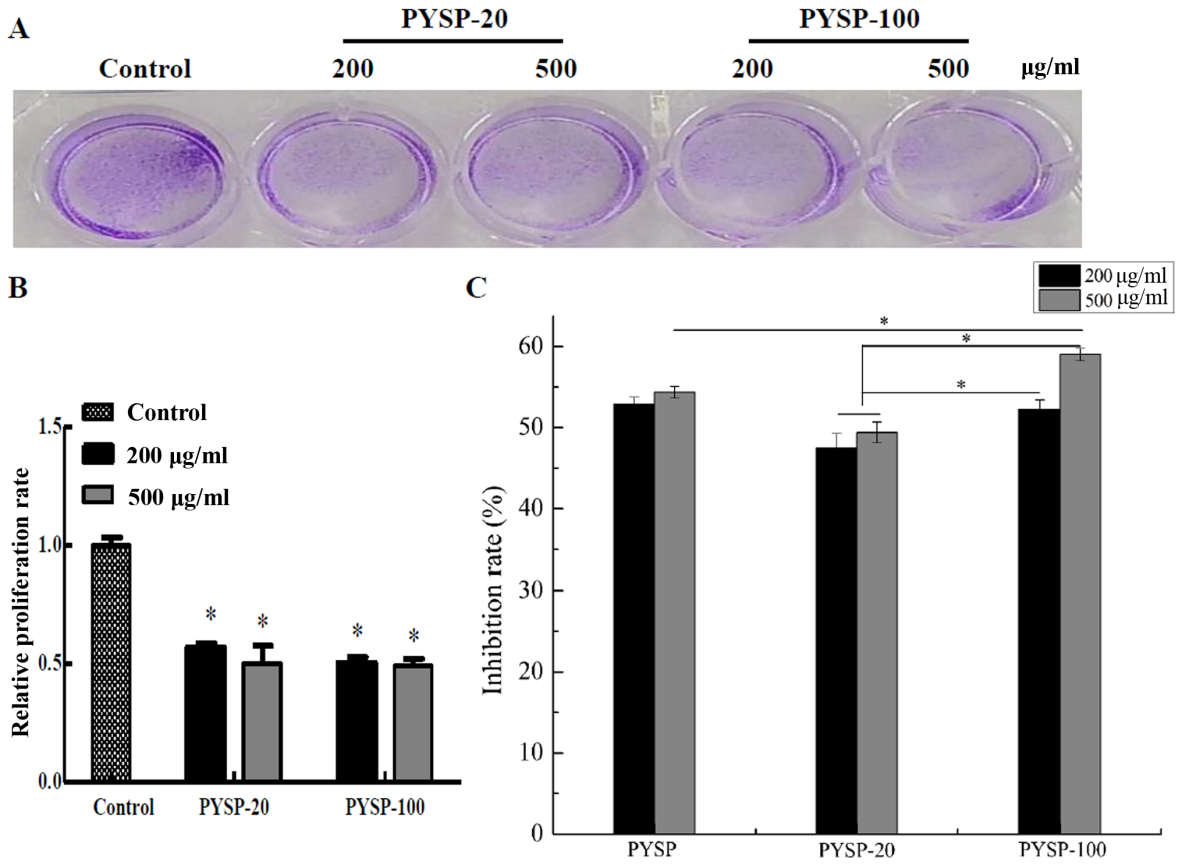

Figure 5. Effects of polysaccharides on Hep3B cell proliferation. (A) Crystal violet staining images. (B) Relative proliferation rate, as measured by crystal violet staining (n=3). Stastical analysis was performed using one-way ANOVA followed by Tukey's post hoc test. *P<0.05 vs. control. (C) Inhibition rate as measured by MTT assay. Data are the means ± SD (n=3). Stastical analysis was performed using two-way ANOVA followed by Tukey's post hoc test. *P<0.05. PYSP, sulfated polysaccharide extracted from *P. yezoensis* Sookwawon 104; PYSP-20, degradation product of PYSP obtained using 20 kGy gamma-irradiation; PYSP-100, degradation product of PYSP obtained using 100 kGy gamma-irradiation.

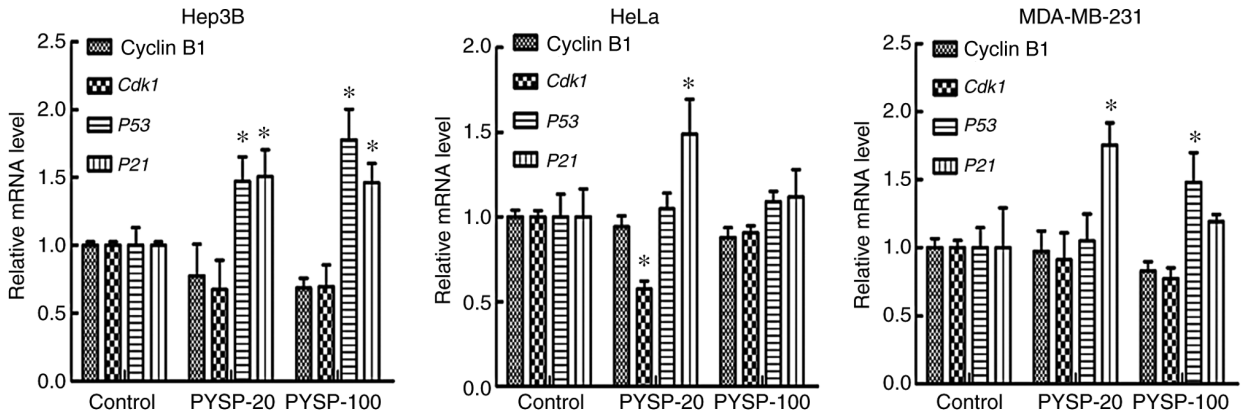

Figure 6. Effects of PYSP-20 and PYSP-100 on gene expression associated with the cell cycle. Data are expressed as means ± SD (n=3). Stastical analysis was performed using one-way ANOVA followed by Tukey's post hoc test. *P<0.05 vs. control. PYSP-20, degradation product of PYSP obtained using 20 kGy gamma-irradiation; PYSP-100, degradation product of PYSP obtained using 100 kGy gamma-irradiation; PYSP, sulfated polysaccharide extracted from *P. yezoensis* Sookwawon 104.

bioavailability of polysaccharides (30), a degradation method using gamma-irradiation was used to prepare low-Mw polysaccharides from PYSP using the irradiation doses 20 and 100 kGy, according to our previous studies (15,31,32). In the present study, PYSP-20 and PYSP-100 exhibited a significant reduction in Mw compared with PYSP, but the monosaccharide composition and sulfate group content did not change markedly, consistent with our previous study (32). In addition, in the FT-IR spectra, there was also no clear difference in the characteristic absorption bands among these polysaccharides, the only exception being that PYSP-20 and PYSP-100 exhibited a slight difference in the stretching vibrations of carboxyl and carbonyl groups, possibly due to the breaking of those chemical bonds by the gamma-irradiation (32).

Polysaccharides have been shown to exhibit lower inhibition rates on tumor cells when used at low concentrations. For example, a polysaccharide from *Cordyceps gunnii* mycelia demonstrated only weak inhibitory activity against tumor cells when used at a low concentration, such as 50 or 100 μg/ml (33). Zhang *et al* (34) also demonstrated that low concentrations of polysaccharide, ranging from 25 to 100 μg/ml, had only a weak inhibitory effect on tumor cell viability. Therefore, with consideration of these previous studies, the sample concentrations used in the present study were selected as 200 and 500 μg/ml. PYSP and its derivatives exhibited different Mw distribution ranges, and PYSP with a higher Mw exhibit weaker antitumor capability compared with its low-Mw derivatives (PYSP-20 and PYSP-100). Therefore, we speculate that Mw is a key factor affecting the distinct antiproliferative activity of PYSP and its derivatives. This is consistent with a previous study (35), in which the Mw of sulfated *Artemisia sphaerocephala* polysaccharides was highly associated with their antitumor activity, and low-Mw polysaccharide demonstrated a greater inhibitory ability against A549, HepG2 and HeLa cells *in vitro*. However, for the HeLa cells in the present study, the high-Mw polysaccharide PYSP exhibited antiproliferative activity only at the lower concentration, indicating that the antiproliferative activity of high-Mw polysaccharide might also be affected by the dosage. Choromanska *et al* (36) demonstrated that high-Mw β-glucan had stronger growth inhibitory activity against A549 and H69AR cells at a low concentration (200 μg/ml) compared with other higher concentrations. Although these results indicate that the low-Mw polysaccharides in the present study have a promising *in vitro* antiproliferative effect on cancer cell lines, validation of their antitumor effect and evaluation of toxicity are required in further studies. Also, previous studies have demonstrated that the upregulation of *P53* and *P21*, together with the downregulation of Cyclin B1 and *Cdk1*, serve important roles in blocking the cell cycle, which is the potential antitumor mechanism of a variety of clinical anticancer medicines (37-40). The present data demonstrate that PYSP-20 and PYSP-100 are able to regulate the expression of *P53*, *P21*, Cyclin B1 and *Cdk1* and so may induce cell cycle arrest. As was shown above the studies have shown that polysaccharides have antitumor activity. Meanwhile, it was reported that polysaccharide was also a kind chemotherapeutic assistant drug. For example, one study reported that when low-Mw polysaccharide was used as a carrier for 5-fluorouracil (5-FU), the antitumor activity of 5-FU against transplanted S180 tumors in mice was enhanced (41). Thus, the synergistic effects of polysaccharide with conventional chemotherapeutic drugs, as a combination therapy against cancer, are of considerable interest.

In summary, a sulfated polysaccharide from *P. yezoensis* Sookwawon 104 and its low-Mw derivatives obtained by gamma irradiation were investigated in the present study. Gamma irradiation did not cause significant changes in the sulfate group content and monosaccharide composition, although changes in the Mw distribution were observed. The *in vitro* antiproliferation assays indicated that Mw had a significant influence on the antitumor activity of the sulfated polysaccharides. The low-Mw polysaccharides exhibited stronger antiproliferative effects than PYSP, and the potential mechanisms may involve cell cycle arrest. Prior to the further research and development of PYSP and its degradation derivatives, strong supporting data from *in vivo* antitumor assays are urgently required. However, the current findings promote the exploitation and utilization of polysaccharide from *P. yezoensis* Sookwawon 104 as a promising candidate for cancer adjuvant therapy.

Acknowledgements

The authors would like to thank Dr Alan K Chang (Wenzhou University; Wenzhou, China) for helpful discussion and for revising the language of the manuscript.

Funding

This study was financially supported by the National Natural Science Foundation of China (grant nos. 41876197 and 81872952), the National Key Research and Development Project (grant no. 2018YFD0901503), the Natural Science Foundation of Zhejiang Province (grant nos. LY18C020006 and LGN18C02 0004), the Scientific Foundation of Education Department of Zhejiang Province (grant no. Y201737374), the National Research Foundation of Korea (grant no. NRF-2018R1D1A1B07049359) and a Golden Seed Project Grant funded by Ministry of Oceans and Fisheries (grant no. 213008-05-4-SB910).

Availability of data and materials

The datasets used and/or analyzed during the current study are available from the corresponding author on reasonable request.

Authors' contributions

DH, LY, YC,XM, SW, JZ and EJP performed the experiments. JL designed the experiments used to evaluate the physicochemical properties. DH, HT, MW and JIC designed the study; DH and HT analyzed the data. DH wrote the original draft of the manuscript, and DH, LY and HT revised it. All authors read and approved the final manuscript.

Ethics approval and consent to participate

Not applicable.

Patient consent for publication

Not applicable.

Competing interests

The authors declare that they have no competing interests.

References

1. Zhang Q, Li N, Zhou G, Lu X, Xu Z and Li Z: In vivo antioxidant activity of polysaccharide fraction from *Porphyra haitanensis* (Rhodephyta) in aging mice. Pharmacol Res 48: 151-155, 2003.
2. Yu X, Zhou C, Yang H, Huang X, Ma H, Qin X and Hu J: Effect of ultrasonic treatment on the degradation and inhibition cancer cell lines of polysaccharides from *Porphyra yezoensis*. Carbohyd Polym 117: 650-656, 2015.

3. Liu QM, Xu SS, Li L, Pan TM, Shi CL, Liu H, Cao MJ, Su WJ and Liu GM: In vitro and in vivo immunomodulatory activity of sulfated polysaccharide from *Porphyra haitanensis*. Carbohyd Polym 165: 189-196, 2017.
4. Varela-Álvarez E, Paulino C and Serrão EA: Development and characterization of twelve microsatellite makers for *Porphyra linearis* Greville. Genetica 145: 127-130, 2017.
5. Venkatraman KL and Mehta A: Health benefits and pharmacological effects of *Porphyra* Species. Plant Foods Hum Nutr 74: 10-17, 2019.
6. Chen YY and Xue YT: Optimization of microwave assisted extraction, chemical characterization and antitumor activities of polysaccharides from *Porphyra haitanensis*. Carbohyd Polym 206: 179-186, 2019.
7. Fernández LE, Valiente OG, Mainardi V, Bello JL, Vélez H and Rosado A: Isolation and characterization of an antitumor active agar-type polysaccharide of *Gracilaria dominguensis*. Carbohyd Res 190: 77-83, 1989.
8. Lins KO, Bezerra DP, Alves AP, Alencar NM, Lima MW, Torres VM, Farias WR, Pessoa C, de Moraes MO and Costa-Lotufo LV: Antitumor properties of a sulfated polysaccharide from the red seaweed *Champia feldmannii* (Diaz-Pifferer). J Appl Toxicol 29: 20-26, 2009.
9. Brown ES, Allsopp PJ, Magee PJ, Gill CI, Nitecki S, Strain CR and McSorley EM: Seaweed and human health. Nutr Rev 72: 205-216, 2014.
10. Cheong KL, Qiu HM, Du H, Liu Y and Khan BM: Oligosaccharides derived from red seaweed: Production, properties, and potential health and cosmetic application. Molecules 23: 2451, 2018.
11. Taper HS and Roberfroid MB: Inulin/oligofructose and anticancer therapy. Br J Nutr 87 (Suppl 2): S283-S286, 2002.
12. Ferro V, Dredge K, Liu L, Hammond E, Bytheway I, Li C, Johnstone K, Karoli T, Davis K, Copeman E and Gautam A: PI-88 and novel heparan sulfate mimetics inhibit angiogenesis. Semin Thromb Hemost 33: 557-568, 2007.
13. Vetvicka V: Synthetic oligosaccharides-clinical application in cancer therapy. Anticancer Agents Med Chem 13: 720-724, 2013.
14. Zhao T, Zhang Q, Qi H, Zhang H, Niu X, Xu Z and Li Z: Degradation of porphyran from *Porphyra haitanensis* and the antioxidant activities of the degraded porphyrans with different molecular weight. Int J Biol Macromol 38: 45-50, 2006.
15. Choi JI and Kim HJ: Preparation of low molecular weight fucoidan by gamma-irradiation and its anticancer activity. Carbohyd Polym 97: 358-362, 2013.
16. Yanagido A, Ueno M, Jiang Z, Cho K, Yamaguchi K, Kim D and Oda T: Increase in anti-inflammatory activities of radical-degraded porphyrans isolated from discolored nori (*Pyropia yezoensis*). Int J Biol Macromol 117: 78-86, 2018.
17. Saruchi, Kumar V, Mittal H and Alhassan SM: Biodegradable hydrogels of tragacanth gum polysaccharide to improve water retention capacity of soil and environment-friendly controlled release of agrochemicals. Int J Biol Macromol 132: 1252-1261, 2019.
18. Ma XL, Song FF, Zhang H, Huan X and Li SY: Compositional monosaccharide analysis of Morus nigra Linn by HPLC and HPCE quantitative determination and comparison of polysaccharide from Morus nigra Linn by HPCE and HPLC. Curr Pharma Anal 13: 433-437, 2017.
19. Dubois M, Gilles KA, Hamilton JK, Rebers PA and Smith F: Colorimetric method for determination of sugars and related substances. Anal Chem 28: 350-356, 1956.
20. Bradford MM: A rapid and sensitive method for the quantitation of microgram quantities of protein utilizing the principle of protein-dye binding. Anal Biochem 72: 248-254, 1976.
21. Dodgson KS and Price RG: A note on the determination of the ester sulphate content of sulphated polysaccharides. Biochem J 84: 106-110, 1962.
22. Wu S, Zhang X, Liu J, Song J, Yu P, Chen P, Liao Z, Wu M and Tong H: Physicochemical characterization of *Sargassum fusiforme* fucoidan fractions and their antagonistic effect against P-selectin-mediated cell adhesion. Int J Biol Macromol 133: 656-662, 2019.
23. Chen L, Chen P, Liu J, Hu C, Yang S, He D, Yu P, Wu M and Zhang X: *Sargassum fusiforme* polysaccharide SFP-F2 activates the NF-κB signaling pathway via CD14/IKK and P38 Axes in raw264.7 cells. Mar Drugs 16: 264, 2018.
24. Chen P, He D, Zhang Y, Yang S, Chen L, Wang S, Zou H, Liao Z, Zhang X and Wu M: *Sargassum fusiforme* polysaccharides activate antioxidant defense by promoting Nrf2-dependent cytoprotection and ameliorate stress insult during aging. Food Funct 7: 4576-4588, 2016.
25. Livak KJ and Schmittgen TD: Analysis of relative gene expression data using real-time quantitative PCR and the 2(-Delta Delta C(T)) method. Methods 25: 402-408, 2001.
26. Alboofetileh M, Rezaei M, Tabarsa M, Rittà M, Donalisio M, Mariatti F, You S, Lembo D and Cravotto G: Effect of different non-conventional extraction methods on the antibacterial and antiviral activity of fucoidans extracted from *Nizamuddinia zanardinii*. Int J Biol Macromol 124: 131-137, 2019.
27. Xia YG, Wang TL, Yu SM, Liang J and Kuang HX: Structural characteristics and hepatoprotective potential of *Aralia elata* root bark polysaccharides and their effects on SCFAs produced by intestinal flora metabolism. Carbohyd Polym 207: 256-265, 2019.
28. Liu C, Omer AM and Ouyang XK: Adsorptive removal of cationic methylene blue dye using carboxymethyl cellulose/k-carrageenan/activated montmorillonite composite beads: Isotherm and kinetic studies. Int J Biol Macromol 106: 823-833, 2018.
29. Cao J, Wang J, Wang S and Xu X: *Porphyra* species: A mini-review of its pharmacological and nutritional properties. J Med Food 19: 111-119, 2016.
30. Babin JL, Traylor KL and Witt DM: Laboratory monitoring of low-molecular-weight heparin and fondaparinux. Semin Thromb Hemost 43: 261-269, 2017.
31. Choi JI, Kim HJ and Lee JW: Structural feature and antioxidant activity of low molecular weight laminarin degraded by gamma irradiation. Food Chem 129: 520-523, 2011.
32. Choi JI, Lee SG, Han SJ, Cho MH and Lee PC: Effect of gamma irradiation on the structure of fucoidan. Radiat Phys Chem 100: 54-58, 2014.
33. Zhu ZY, Dong F, Liu X, Lv Q, YingYang, Liu F, Chen L, Wang T, Wang Z and Zhang Y: Effects of extraction methods on the yield, chemical structure and anti-tumor activity of polysaccharides from *Cordyceps gunnii* mycelia. Carbohydr Polym 140: 461-471, 2016.
34. Zhang Y, Wang Z, Li D, Zang W, Zhu H, Wu P, Mei Y and Liang Y: A polysaccharide from *Antrodia cinnamomea* mycelia exerts antitumor activity through blocking of TOP1/TDP1-mediated DNA repair pathway. Int J Biol Macromol 120B: 1551-1560, 2018.
35. Wang J, Bao A, Meng X, Guo H, Zhang Y, Zhao Y, Kong W, Liang J, Yao J and Zhang J: An efficient approach to prepare sulfated polysaccharide and evaluation of anti-tumor activities in vitro. Carbohyd Polyms 184: 366-375, 2018.
36. Choromanska A, Kulbacka J, Harasym J, Oledzki R, Szewczyk A and Saczko J: High- and low-molecular weight oat Beta-glucan reveals antitumor activity in human epithelial lung cancer. Pathol Oncol Res 24: 583-592, 2018.
37. Pletenpol JA and Stewart ZA: Cell cycle checkpoint signaling: Cell cycle arrest versus apoptosis. Toxicology 181-182: 475-481, 2002.
38. Wang J, Zhang YS, Thakur K, Hussain SS, Zhang JG, Xiao GR and Wei ZJ: Licochalcone A from licorice root, an inhibitor of human hepatoma cell growth via induction of cell apoptosis and cell cycle arrest. Food Chem Toxicol 120: 407-417, 2018.
39. Zhao H, Li S, Wang G, Zhao W, Zhang D, Wang F, Li W and Sun L: Study of the mechanism by which dinaciclib induces apoptosis and cell cycle arrest of lymphoma Raji cells through a CDK1-involved pathway. Cancer Med 8: 4348-4358, 2019.
40. Khan T, Date A, Chawda H and Patel K: Polysaccharides as potential anticancer agents-A review of their progress. Carbohyd Polyms 210: 412-428, 2019.
41. Wang X and Zhang Z: The antitumor activity of a red alga polysaccharide complexes carrying 5-fluorouracil. Int J Biol Macromol 69: 542-545, 2014.